

# Structure of Heat-Treated Nylon 6 and 6.6 Fibers. I. The Shrinkage Mechanism

ABIGAIL LISBÃO SIMAL, ADRIANA REGINA MARTIN

Departamento de Engenharia de Materiais, Universidade Federal de São Carlos, Via Washington Luiz, Km. 235, Caixa Postal 676, 13565-905 São Carlos, SP, Brazil

Received 17 June 1997; accepted 9 October 1997

**ABSTRACT:** Nylon 6 and 6.6 fibers were submitted to thermal annealing in a wide range of temperatures (below and above their glass transition temperatures) under inert atmosphere and slack condition, allowing free shrinkage. The structural changes due to the heat settings were analyzed by several techniques (differential scanning calorimetry analysis, wide- and small-angle X-ray scattering, and birefringence). The results revealed different recrystallization responses of the fibers to the applied thermal annealings and consequently different shrinkage mechanisms. In the recrystallization of the Nylon 6 fibers were involved a generation of nuclei crystallites in the interfibrillar regions, as well as growth and perfection of these new crystallites and preexisting ones. But, recrystallization of the Nylon 6.6 fiber was accompanied only by growth and perfection of the preexisting crystals. The existence of the nuclei crystallites at temperatures of heat treatments above 120°C was the major commanding factor for the Nylon 6 fiber to undergo less shrinkage than the Nylon 6.6 fiber. These very tiny crystallites worked as crosslinking points that would impose restrictions in the mobility of the chains segments, inhibiting subsequent disorientation of the amorphous regions and consequently intense shrinkage, thus resulting in recrystallization in a preferred direction of the fiber axis. The Nylon 6.6 fiber experienced an instantaneous shrinkage at the annealing temperature around 70°C. That was the temperature necessary to release its hydrogen bonds and the starting temperature for presenting its major structural changes, including global disorientation of the amorphous and crystalline regions. Thus, its recrystallization occurred with no preferred orientation. Also, it was suggested that the occurrence of so different shrinkage mechanisms reside in the different crystalline morphology that these fibers originally possessed before the heat treatments. © 1998 John Wiley & Sons, Inc. *J Appl Polym Sci* 68: 441–452, 1998

**Key words:** Nylon 6; Nylon 6.6; shrinkage mechanism; fibers; heat treatment

## INTRODUCTION

The processing conditions, such as heat and humidity of synthetic fibers, have significant influence on several properties of interest (mechanical behavior, dimensional stability, and dyeability),

and consequently on their final applications. The structural basis for these changes in the performance of the material can be studied in the laboratory by controlled annealing of the specimens.<sup>1</sup> Therefore, the study of the structural modifications of synthetic fibers due to different heat settings in a laboratorial scale is of great interest.

To analyze the structural modifications in synthetic fibers due to different thermal treatments, several parameters are studied, and the possibility of a relationship among them is compared. The most commonly studied parameters are the

---

Correspondence to: A. L. Simal.

Contract grant sponsor: CAPES; contract grant sponsor: FAPESP.

*Journal of Applied Polymer Science*, Vol. 68, 441–452 (1998)

© 1998 John Wiley & Sons, Inc.

CCC 0021-8995/98/030441-12

shrinkage and crystallinity percentages, size and perfection of the crystals, as well as long periods and orientation.<sup>2</sup>

The shrinkage parameter, for example, can give us valuable information about the thermal history of synthetic fibers. It has been shown in the literature<sup>3</sup> that the shrinkage process can be associated with two phenomena: disorientation of the noncrystalline chains and recrystallization. More recently, Fouda and colleagues<sup>4</sup> have associated the structural changes due to thermal annealing to the occurrence of the following phenomena: disorientation; recrystallization by nucleation and growth; and shrinkage and crystal decomposition. The extent of occurrence of each one or all of these phenomena will depend on the annealing conditions, mainly time and temperature.

Yet, other authors<sup>5</sup> have shown the appearance of a middle endotherm in differential scanning calorimetry (DSC) thermograms for poly(ethylene terephthalate) (PET) fibers, which have been submitted to different heat setting conditions. These middle endotherms have been related to the fusion of nuclei crystallites that have been developed within the extended amorphous regions of these fibers during annealing. Also, these authors<sup>5</sup> have proposed that the formation of such nuclei crystallites will prevent the complete disorientation of the amorphous region, therefore controlling the amount of shrinkage of this fiber at temperatures of heat treatment above its glass transition temperature ( $T_g$ ). A similar result has been shown by Khanna<sup>6</sup> for Nylon 6 fibers.

Although the appearance of such a middle endotherm in DSC thermograms has been described mainly for heat-treated PET fibers,<sup>5,7,8</sup> its appearance in Nylon 6 fibers<sup>6</sup> suggests that this phenomena might be a more general one, possibly occurring in other heat-treated synthetic fibers. To verify this hypothesis and its relationship to the shrinkage behavior of different synthetic fibers, Nylon 6.6 fibers were submitted to a wide range of temperatures of heat treatments. This fiber was chosen because it is a very important industrial fiber and has some structural similarities to the Nylon 6 ones, thus allowing better comparison. Therefore, in addition, Nylon 6 fibers were submitted to the same conditions of heat treatments, and the results are reported.

Yet, to accomplish such study, several structural characterization techniques were applied: X-ray diffraction (small- and wide-angle), DSC, dynamic and mechanical thermal analysis (DMTA), and polarized light optical microscopy. These

techniques were demonstrated to be not only essential, but also complementary to each other, and also to promote the necessary understanding of the structural changes of these fibers due to thermal annealing.

## EXPERIMENTAL

### Sample Preparation

Nylon 6 and 6.6 fibers from De Millus S/A (Rio de Janeiro, Brazil) and Rhodia S/A (Santo André, SP, Brazil), respectively, were submitted to dry heat settings under slack conditions in an evacuated oven under an inert atmosphere. The inert atmosphere was applied to avoid thermal decomposition of the fibers, as described by some authors.<sup>4</sup> The fibers were heat-treated for 2 h in the following temperatures: 70, 80, 100, 120, 135, 150, 170, 180, and  $190 \pm 2^\circ\text{C}$ . After the heat treatments, the fibers remained in the desiccator for 30 days before data collection. The time of 2 h was chosen based on two previous work by one of the authors.<sup>2,9</sup>

Although the fibers were processed by different conditions (different sources), they present the same level of draw ratios:  $3.2 \times$  for Nylon 6 and  $3.29 \times$  for Nylon 6.6. The spinning and drawing processes for Nylon 6 were continuous, whereas for Nylon 6.6 they were discontinued. Nylon 6 and 6.6 were presented as multifilament fibers, with 6 and 23 filaments, respectively.

### Structural Measurements

#### Shrinkage

Shrinkage measurements were made by knowing the length before and after the heat treatments under slack conditions.

Therefore, the shrinkage percentage ( $\%S_h$ ) was calculated through the following expression:

$$\%S_h = \frac{S_h^0 - S_h^f}{S_h^0} \times 100 \quad (1)$$

where  $S_h^0$  and  $S_h^f$  are the initial and final lengths, respectively.

#### DSC

DSC (from Perkin–Elmer, Norwalk, CT) measurements were used to obtain the thermograms and calculate the crystallinities from the observed

areas under the heat of fusion peaks ( $\Delta H_f$ ) of the samples. The crystallinity percentages (%C) were calculated as follows:

$$\%C = \frac{\Delta H_f}{\Delta H_0} \times 100 \quad (2)$$

where  $\Delta H_0$  are the values of the heat of fusion for the totally crystalline Nylon 6 and 6.6 with  $\alpha$ -phase, or  $166.5 \text{ J/g}^{-1}$ ,<sup>10</sup> and  $191.0 \text{ J/g}^{-1}$ ,<sup>11</sup> respectively.  $\Delta H_f$  is the observed heat of fusion in Joules per gram.

The runnings were effectuated under inert atmosphere at a heating rate of  $10^\circ\text{C min}^{-1}$ .

### DMTA

DMTA (from Polymer Laboratories, England) runnings were used to evaluate the  $T_g$  of the samples taken where  $E''$  is maximum. The running conditions were: heating rate of  $3^\circ\text{C min}^{-1}$  and frequency of 10 Hz.

### X-Ray Analysis

Wide-angle X-ray scattering was performed in a Rigaku Rotaflex diffractometer, model R1-200B, using a Ni-filtered  $\text{CuK}\alpha$  radiation.

The obtained diffractograms were used to calculate the crystal size (CS) and lateral order (LO).

Our Nylon 6 and 6.6 fibers presented a characteristic two-peak equatorial X-ray scattering pattern for an  $\alpha$ -structure as described by several authors<sup>1,12,13</sup> before and after heat treatments. The observed peak maximas for Nylon 6 fibers were:  $2\theta_1 \cong 20.28^\circ$  and  $2\theta_2 \cong 23.14^\circ$ , which correspond to the reflection planes (002) and (200), respectively, and for Nylon 6.6 fibers were:  $2\theta_1 \cong 20.5^\circ$  and  $2\theta_2 \cong 22.9^\circ$  corresponding to the reflection planes (100) and (010), respectively.

CSs<sup>1,14</sup> were calculated using the Scherrer equation or

$$CS = \frac{K\lambda}{\beta(\cos \theta)} \quad (3)$$

where  $K$  is the shape factor that varies between 0.9 to 1.1 (a value of 0.90<sup>1</sup> has been considered for our calculations),  $\lambda$  is the wavelength of the radiation used ( $\text{CuK}\alpha = 1.5418 \text{ \AA}$ ),  $\beta$  is the half-maximum breath in radians, and  $\theta$  is Bragg's angle.

The crystalline size measurement corresponds to the direction perpendicular to the plane consid-

ered for the calculations. For instance, the (200) and (100) reflections were used to obtain the sizes along the hydrogen bonded direction, and the (002) and (010) correspond to the size along the Van der Waals bonded direction for Nylon 6<sup>1</sup> and 6.6,<sup>15</sup> respectively.

The half-maximum breath of these reflections were obtained after deconvolution of the X-ray diffractograms. Finally, the calculated values of the CS should be considered as relative values only, because the necessary corrections for the Scherrer equation<sup>14</sup> were not made.

The LO<sup>7,13</sup> parameter can be related to several factors at same time, such as the crystallinity of the samples, perfection, size, and distribution of the crystallites; it was calculated from the following equation:

$$\%LO = (1 - RF) \times 100 \quad (4)$$

where  $RF$  is the resolution factor, which is given by the following expression for the case of the nylons<sup>7,13</sup>:

$$RF = \frac{2m}{h_1 + h_2} \quad (5)$$

where  $m$  is the height of the minimum from the appropriate base line, and  $h_1$ ,  $h_2$  are the heights of the maxima from the same base line.<sup>13</sup> Therefore,  $m$  corresponds to the minima between the two reflections peaks representing Nylon 6 and 6.6 fibers.

Some authors<sup>13</sup> have used this parameter in substitution with the crystalline index measurement. In this case, it is being considered the total order rather than the absolute crystallinity of the sample, due its dependence to several crystalline parameters as already explained.

Small-angle X-ray scattering was performed in a Statton Camera<sup>14</sup> fixed in a Phillips system, model MW 1130/00/60, using a Rotatory anode (Ni-filtered radiation). It was used a pinhole collimation with a specimen to film distance of 29 cm and an exposure time of 24 h. The long period distance was calculated from the meridional diffraction patterns using the Bragg equation as described elsewhere.<sup>14</sup>

### Birefringence

Birefringence ( $\Delta n$ ) was measured by polarized light microscopy (Leitz SM, Lux-POL) using a Be-

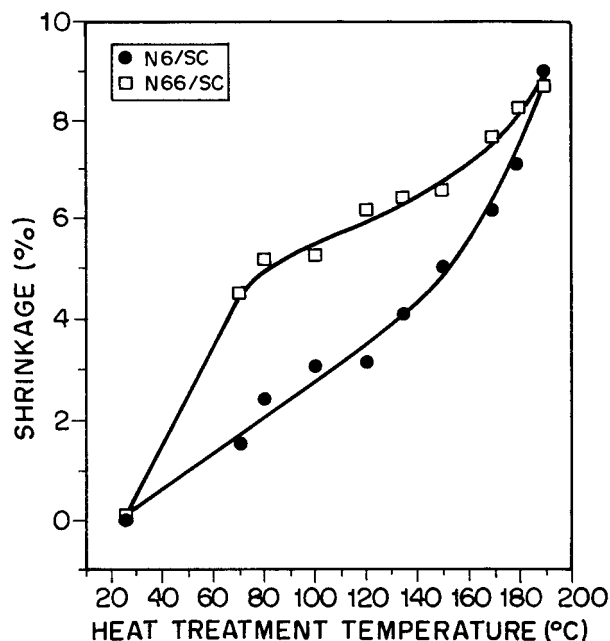


**Figure 1** Shrinkage percentage vs. annealing temperatures for the Nylon 6 (●) and Nylon 6.6 (□) fibers. N6, Nylon 6; N66, Nylon 6.6; SC, heat treated under slack condition.

reck compensator. The same microscope was used to measure the diameter of the fibers.

## RESULTS AND DISCUSSION

### Differences in Shrinkage Behavior

Figure 1 compares the shrinkage behavior of Nylon 6 and 6.6 fibers as the temperature of heat treatment increases.

It can be seen that the Nylon 6 fiber shrinks less and more gradually than the Nylon 6.6 fiber for most of the analyzed temperatures, thus reaching the same level of shrinkage of the Nylon 6.6 fiber only at a temperature of heat treatment of 190°C. Although Nylon 6.6 presented a higher  $T_g$  than the Nylon 6 (115°C and 96°C for the control fibers, respectively), it seems that the thermal energy necessary to promote effective shrinkage will be reached more easily for Nylon 6.6 at temperatures of heat treatment around its  $T_g$ . Nylon 6 will be shrinking more intensively only at temperatures above 150°C, which is well above its  $T_g$ . At a temperature around 70°C, Nylon 6.6 has already shrunk 51% of its shrinkage value reached at a temperature of 190°C, whereas Nylon

6 will be reaching the same percentage of shrinkage only at temperature around 150°C.

Therefore, the existence of chain flexibility for Nylon 6.6 seems to be essential to overcome their strong hydrogen bonds and probably is the major controlling factor for its shrinkage behavior. However, other factors, in addition to chain flexibility, might be playing a role in the shrinkage behavior of the Nylon 6 fiber.

Thus, to understand better these differences in the shrinkage behavior between these fibers, the following discussion will be relevant.

When drawn fibers are submitted to increased annealing temperatures and are allowed to shrink freely for a fixed time, one could expect the occurrence of two processes: the partial disorientation of the noncrystalline chains and recrystallization associated with an increase of crystallinity, size, and perfection of crystals.

The amount of disorientation of the amorphous regions will depend on the annealing temperature and time.<sup>3</sup> This disorientation is associated with the molecular relaxation to alleviate preexisting tensions due to processing (spinning and drawing). As the temperature of the heat treatment increases, the molecules gain mobility and will tend to acquire a conformation of lower energy, which is more stable. Such conformation will be reached when the segments of the macromolecules loose orientation. The amount of disorientation in the noncrystalline chains with increasing temperature will be proportional to the shrinkage that occurred in the sample.<sup>3</sup> Also, the amount of shrinkage will depend on the initial structure present in the original drawn fibers before the annealing.

As the disorientation proceeds, simultaneous recrystallization will take place. This recrystallization process will be favored by an increase in the annealing temperature, especially at a temperature above the  $T_g$  of the fibers, due to the existence of intense mobility of the macromolecular chains.

By recrystallization, one understands increase of crystallinity through a generation of new crystallites and an increase of size and perfection of the preexisting crystals.<sup>4</sup>

### Differences in the Recrystallization Process

Analyzing our DSC thermograms (Figure 2), we observed the appearance of a small endotherm (premelting peak) in addition to the characteristic main endotherm, only for the Nylon 6 fibers.

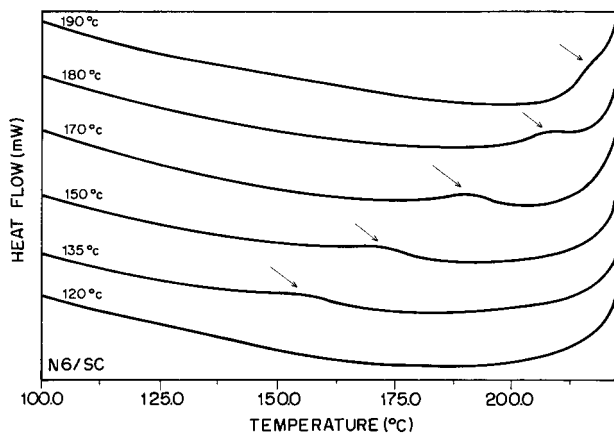


**Figure 2** DSC thermograms of the Nylon 6 fibers at several annealing temperatures. Arrows indicate the premelting temperatures. N6, Nylon 6; SC, change for heat treated under slack condition.

The appearance of this endotherm has been described by other authors<sup>5-8</sup> for PET and Nylon 6 fibers when submitted to different annealing conditions.

Also, there seems to be a general agreement concerning the nature of such an endotherm. It has been referred<sup>5,8</sup> to as the melting of the new crystallites (nuclei crystallites) formed in the amorphous regions of the fibers during the heat-setting process.

Considering the three phases model described in the literature<sup>16</sup> for the melt spun and drawn fibers, which consist of a sequence of amorphous and crystalline domains (called microfibrils) and extended noncrystalline molecules (interfibrillar matter) to represent the morphology of the PET and Nylon fibers, these microcrystallites are believed to be located in the interfibrillar regions.<sup>5,6</sup>

Also, Figure 2 reveals that this endotherm, although very small, starts to be visible only for the heat treatments realized above 120°C.

In addition, Figure 3 indicates that the temperature where this endotherm occurs increases linearly with the increase in annealing temperature.

Similar results have been described in the literature for PET<sup>5</sup> and Nylon 6<sup>6</sup> fibers. Therefore, the increase in the heat-setting temperature seems to enhance the perfection and size of these new microcrystallites, which would be responsible for the observed dislocation of the temperature of this new endotherm to higher temperatures.

Another interesting observation is that the temperatures of these endotherms are occurring in a temperature range of 20 to 25°C above the corresponding temperatures of the applied heat

treatments. This behavior has been referred by some authors<sup>8</sup> as the ultimate temperature where the fibers could present thermal stability (i.e., the heat-setted fibers) and would present structural stability up to temperatures around 20 to 25°C above the annealing temperature.

The absence of such a new endotherm in the Nylon 6.6 fibers indicates that the heat treatments are affecting differently the structure of the studied nylons and consequently their shrinkage behavior. As described previously, the initial structure presented in the control fibers (not previously heat treated) can be one of the contributing factors for such a differentiated response to the heat setting. Although the analyzed fibers have similar draw ratios and their processing resulted in an  $\alpha$ -structure, they presented some inherent structural differences. Some of these differences are: the length of their chain-repeated unit and the type of their unit cells.

Other structural differences can be visualized in Figure 4.

Figure 4 compares the DSC thermograms before and after the heat settings, for both fibers. As can be seen, the nonheat-treated Nylon 6.6 fibers (control) presented two main endotherms (i.e., a double melting peak), while the control

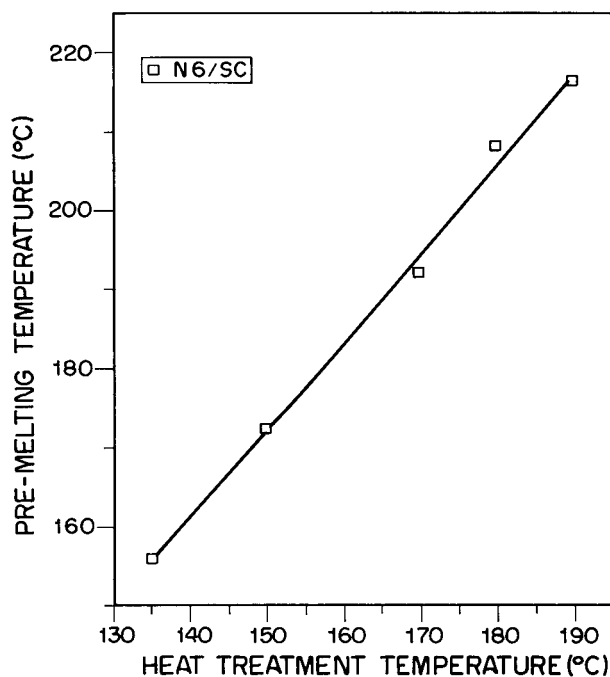


**Figure 3** Linear dependence of the pre-melting temperatures with the annealing temperatures for the Nylon 6 fiber. N6, Nylon 6; SC, heat treated under slack condition.

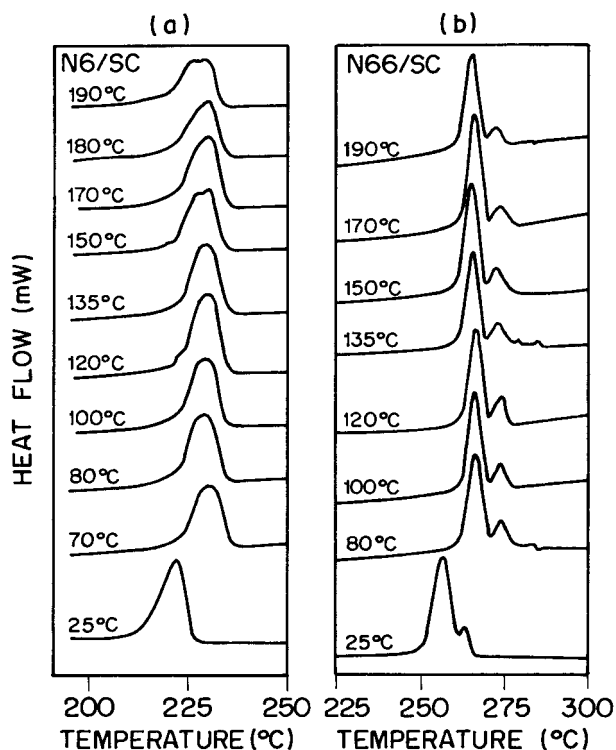


**Figure 4** DSC thermograms of the main melting peaks at several annealing temperatures for the Nylon 6 (a) and Nylon 6.6 (b) fibers. N6, Nylon 6; N66, Nylon 6.6; SC, change for heat treated under slack condition.

Nylon 6 presented only one. Although there is some controversy concerning the appearance of such double melting peaks in Nylon 6.6 fibers by DSC analysis,<sup>17</sup> the maintenance of these double melting peaks as the temperature of the heat treatment is raised strongly reinforces the idea that the original structure of the Nylon 6.6 fibers is composed of two different crystalline structures, as described previously in the literature<sup>17</sup>; but, in our case, they would be probably the same type, but with different degrees of perfection or sizes. Also, Figure 4 does not show evidence for the occurrence of such double melting peaks for the Nylon 6 fibers until the heat treatment temperature of 120°C. However, above this temperature, it becomes clear some tendency of this main endotherm peak to dismember in two peaks. This tendency seems to have some relationship with the occurrence of the premelting peaks in these Nylon 6 fibers in the same range of temperatures of the applied heat treatments. It seems that, at higher annealing temperature, the crystalline structure of the Nylon 6 fibers is becoming more similar to the observed one for the Nylon 6.6 fiber.

Thus the recrystallization process associated

with shrinkage occurred in a different manner for the studied nylons. In the Nylon 6 case, the mobility of the chain segments (especially at high temperatures of heat setting) favors the formation of small crystallites (nuclei crystallites) within the extended noncrystalline chains (interfibrillar regions) and simultaneously promotes changes in the existing crystals (growth and perfection). In the Nylon 6.6 case, the main characteristics of the original crystalline structure seem to be preserved with the applied heat treatments. The major transformations due to the heat settings are those related to growth and perfection of the pre-existing crystals.

#### Relationships between Shrinkage Behavior and the Recrystallization Process

To understand better the observed differences in the recrystallization process between the studied nylons, the parameters associated with the crystalline regions [%C, LO, long period (LP), and CS] were analyzed as a function of the shrinkage percentage.

Figures 5–7 show clearly the linear dependency among these parameters presenting two well-defined linearity regions. This fact confirms the correlation between shrinkage and the recrystallization process as the annealing temperature increases. Also, all analyzed parameters presented a discontinuity around the  $T_g$  of the fibers that separates the two linearity regions. It is evident from these figures that the structural changes at high temperatures of heat treatments are much more intense. Finally, these figures reveal the differences in the recrystallization behavior between the Nylon 6 and 6.6 fibers. Analyzing the crystallinity parameter [Fig. 5(a,b)], it is possible to verify that the two linearity regions are separated by a partial decrease in the crystallinity percentage. This effect is more pronounced for the Nylon 6.6 fiber, and it is occurring at a heat-setting temperature above 80°C. For the Nylon 6 case, it is occurring above the heat-setting temperature of 120°C. Also, it is evident from these figures that the maximum %C reached by the Nylon 6.6 fiber at a temperature of 190°C is very close to its original crystallinity, before the annealing. But the Nylon 6 fiber presented a maximum value of %C at this same temperature of heat treatment (190°C), about 12% higher than its original crystallinity.

These differences become even more evident when the analyzed parameter is the LO, as can

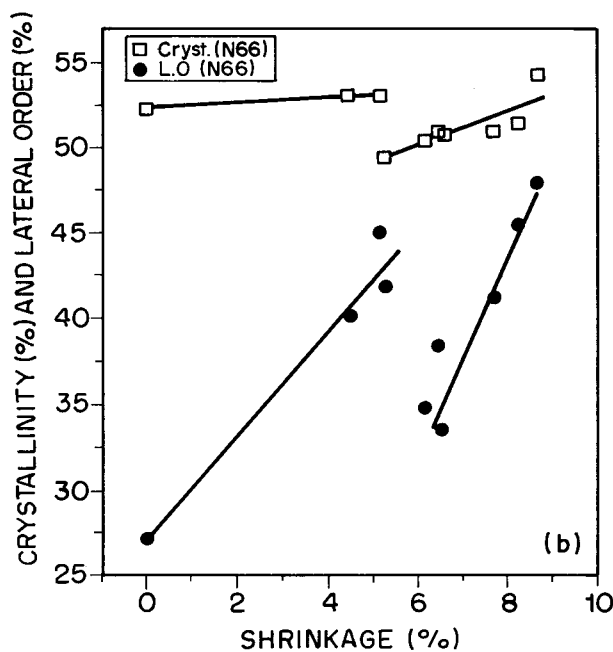
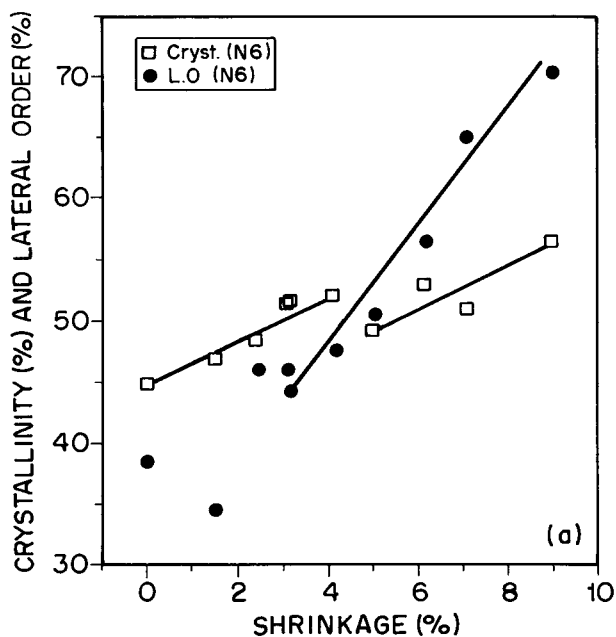


**Figure 5** Crystallinity (Cryst.) percentage and LO (L.O) percentage vs. shrinkage percentage for the Nylon 6 (a) and Nylon 6.6 (b) fibers. N6, Nylon 6; N66, Nylon 6.6.

be seen in the same figures. The LO parameter represents the total order of the system, rather than the absolute crystallinity.<sup>13</sup> It is related to several factors (such as crystallinity, perfection, size, and distribution of the crystals). Again, two linearity regions appear for both fibers, but the

discontinuities regions behave differently. For Nylon 6, the discontinuity region is accompanied by a deep decrease in the LO parameter, following the same pattern as described for the crystallinity parameter, whereas for the Nylon 6 fiber, discontinuity seems to be occurring by a change in the slope only, at temperature of heat treatment around 120°C. These changes in the behavior patterns in the discontinuities regions for the Nylon 6 fiber might be reflecting the conceptual differences between the two analyzed parameters (%C measured by DSC and LO measured by X-ray scattering), as described previously, allowing by this reason a better visualization of the structural response of the different nylons to the applied heat settings.

The partial destruction of the %C is occurring in the vicinity of  $T_g$  for both fibers. Thus, the disorientation process associated with the mobility of the chain segments in the amorphous regions might be contributing for this observed decrease in %C. But, in the case of the Nylon 6 fiber, this partial destruction of the %C is not being accompanied by a decrease in the LO parameters, as detected for the Nylon 6.6 fiber. These results seem to be in accordance with the previous discussion based on the analysis of the DSC thermograms.

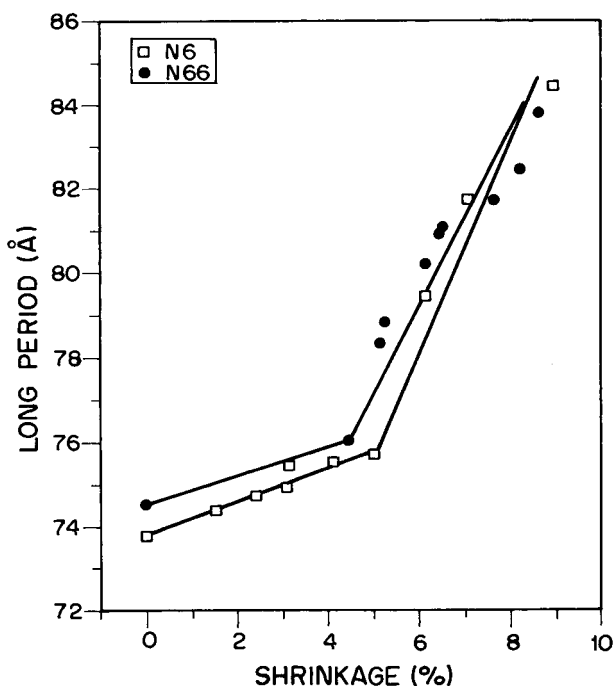


**Figure 6** LP (Å) versus shrinkage percentage for the Nylon 6 (□) and Nylon 6.6 (●) fibers. N6, Nylon 6; N66, Nylon 6.6.

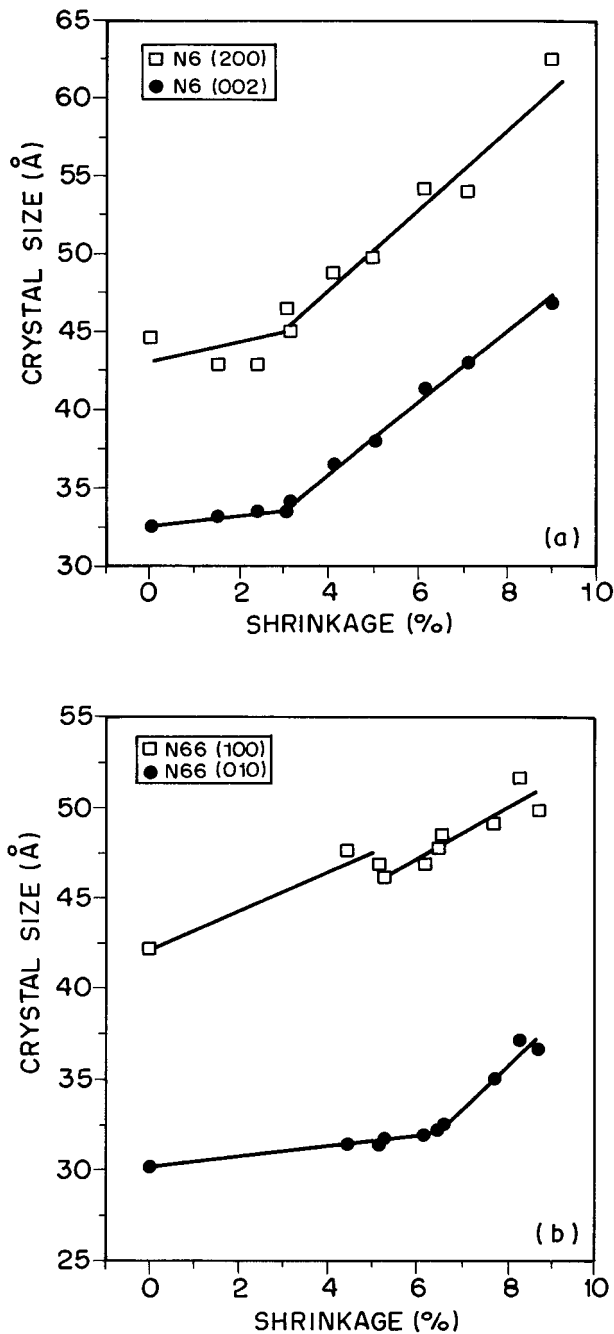


**Figure 7** Crystal sizes (Å) vs. shrinkage percentage for the Nylon 6 (a) and Nylon 6.6 (b) fibers. N6, Nylon 6; N66, Nylon 6.6.

The generation of the very tiny crystallites within the extended noncrystalline regions of the Nylon 6 fibers at annealing temperatures above 120°C might be responsible not only for the observed differences in the LO parameter, but also in the shrinkage behavior when compared with the Nylon 6.6 fiber. For the heat treatments above

120°C, the mobility of the chain segments promotes disorientation and recrystallization simultaneously. Yet, in the recrystallization process, two different phenomena are evolved: the formation of these nuclei crystallites and the increase of size and perfection of the existing crystals. However during thermal annealing, such new crystallites might be acting as crosslinking points that would impose restrictions on the mobility of the chain segments, inhibiting subsequent disorientation of the amorphous regions and consequently intense shrinkage.

A similar result has been suggested by Khanna<sup>6</sup> for his preheat-setted Nylon 6 fiber to describe its thermal mechanical behavior, which underwent less shrinkage than the no-heat-setted one. At a lower range of temperatures of heat treatments (below 120°C), the observed increase in the LO for our Nylon 6 fiber indicates a recrystallization only by improvement of the size and perfection of the existing crystals. But above this temperature, all of the previously described factors will be responsible for the observed increase in the total order of the system.

In the Nylon 6.6 case, the mobility of the chain segments of the amorphous regions is also contributing to the loss of its total order. The deep decrease in the LO parameter in the discontinuity region may be indicating that the disorientation process is not only affecting the amorphous regions, but the crystalline regions as well. Thus, the increase in the LO for the Nylon 6.6 fiber at the range of temperatures below and above its  $T_g$  might be reflecting more the improvement of size and perfection of the preexisting crystals and not the generation of new crystallites. Therefore, the increase in the %C for this fiber, especially at temperatures above its  $T_g$ , is occurring mainly by the reorganization of the preexisting crystalline structure. This fact might be the reason why the maximum in the %C reached by this fiber at 190°C is very close to its original crystallinity, before the applied heat settings. Finally, this reorganization of the original crystalline structure seems to be accompanied by some loss in the global orientation (crystalline plus amorphous orientation). Also, as the DSC thermograms showed, this fiber presented a characteristic double melting peak for all of the temperatures of heat treatments applied, indicating therefore that the basic characteristics of the original crystalline regions are being preserved, reinforcing once more that the increase in crystallinity and LO are reflecting



mainly the growth and perfection of the preexisting crystals.

Figures 6 and 7 confirm the above observations about the increase in the size and perfection of the crystals for both fibers. When the LP—which is a measure of the average repeat distance of the crystals in the direction parallel to the fiber axis—is plotted as a function of the shrinkage percentage (Fig. 6), it is possible to observe that the change in the slope of the two linearity regions is occurring at an annealing temperature of 70°C for Nylon 6.6 and at a temperature of 150°C for Nylon 6. Therefore, a deep increase in this parameter will occur for both fibers only for the heat treatments above these temperatures. This behavior indicates that LP is a direct function of the relaxations of the noncrystalline regions (disorientation) occurring during thermal annealing.

The Nylon 6.6 fiber will experience nearly instantaneous shrinkage (Fig. 1) and consequently a disorientation at temperature around 70°C (about 40°C below its  $T_g$ ). This temperature is coincident with the temperature where LP started to present an accentuated increase as described previously. Also, this seems to be the temperature necessary to overcome the thermal stability imparted by the hydrogen bonds present in this fiber. Above this temperature, the increased segmental mobility of the macromolecules chains will favor the accentuated increase in LP as observed in Figure 6. In the case of Nylon 6, this process will be favored only for the heat treatments above 150°C, which is about 50°C above its  $T_g$ . This fact reflects once again the differences in the recrystallization process between fibers.

The CSs measured in the directions perpendicular to the assigned reflection planes and perpendicular to the fiber axis can be seen in Figure 7. This parameter shows a deep change in the slope around 100°C for the size direction measured along the hydrogen bonds of Nylon 6 and around 70°C for Nylon 6.6. But, this change in the slope is occurring only around 120°C for the size directions measured along the Van der Waals bonds for both fibers. This result seems to indicate that the crystal growth at a direction perpendicular to the planes containing hydrogen bonds will occur only after loosening of such bonds. At a lower range of temperatures, the changes in the CSs in both directions are very small. Also, the necessary energy to overcome such hydrogen bonds is lower for the case of the Nylon 6.6 than for the Nylon 6 fiber. Again, this temperature for Nylon 6.6 coincides with the temperature where it is experienc-

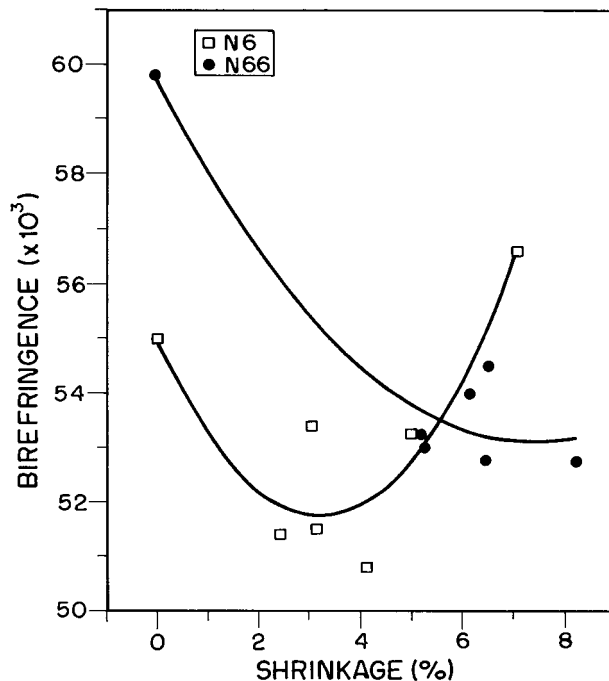


**Figure 8** Birefringence vs. shrinkage percentage for the Nylon 6 (□) and Nylon 6.6 (●) fibers. N6, Nylon 6; N66, Nylon 6.6.

ing instantaneous shrinkage and accentuated changes in the LP parameter. Thus, loosening of the hydrogen bonds seems to play an important role in the shrinkage behavior of the fibers, mainly for the Nylon 6.6 fiber, as described previously.

Nylon 6, as described previously, presented a more complex recrystallization process, wherein generation of the nuclei crystallites seems to be the controlling factor.

Changes in the orientations as described previously for both fibers can be clearly visualized in Figure 8, wherein the birefringence parameter is plotted as a function of the shrinkage percentage. It is well known<sup>2,3</sup> that the  $\Delta n$  parameter measures the total orientation of the samples (i.e., it represents for our nylon fibers the orientation contributions of their amorphous and crystalline regions, as well as their interfibrillar regions).

Figure 8 shows that the  $\Delta n$  decreases deeply at annealing temperatures below the  $T_g$  of the fibers, indicating loss of orientation due to release of tensions at this range of temperature. But, as the shrinkage increases with the annealing temperature, the  $\Delta n$  parameter increases again for the Nylon 6 fiber, presenting a minimum temperature of heat treatment around 120°C. Once more, this minimum is coincident with the temperature

where the nuclei crystallites started to appear for this fiber. Thus, the prevention of a complete disorientation of the interfibrillar regions due to the presence of these new crystallites will favor a global recrystallization in the preferred direction of the axis as the temperature of the heat treatment increases. However, different from the Nylon 6 behavior, the  $\Delta n$  parameter for the Nylon 6.6 fiber is presenting a stabilization for the heat treatments realized above 80°C. Therefore, the nearly instantaneous shrinkage experienced by this fiber at a lower range of annealing temperatures seems to be really affecting, as already discussed, the global orientation of this fiber. Therefore, as the temperature of the heat treatment increases, the recrystallization of the preexisting crystals will be occurring with no preferred orientation (i.e., the improvement of the size and the perfection of the crystals will not affect the  $\Delta n$  values at temperatures of heat setting above 80°C).

## The Proposed Shrinkage Mechanism

### *The Nylon 6 Fiber*

From all of these results, it is possible to establish a shrinkage mechanism for our Nylon 6 fiber, which is very similar to the mechanism proposed by Oswald and colleagues<sup>5</sup> for their PET fibers.

The amount of shrinkage upon thermal treatment must be regarded as the end result of two opposing and competitive processes: one leading to higher entropy and one leading to lower enthalpy of the system.<sup>5</sup> When the temperature of heat treatment exceeds the  $T_g$  of the Nylon 6 fiber, the increased segmental mobility in the oriented amorphous extended chains (interfibrillar region) allows them to seek a state of higher entropy by disorientation (stress relaxation). This event will occur at temperature of heat treatment around 100°C for the Nylon 6 ( $T_g \cong 96^\circ\text{C}$ ) fiber that seems to be the temperature necessary to release its hydrogen bonds. But, this release of strain and the increased segmental mobility as the temperature of the heat treatment increases will favor the formation of the nuclei crystallites, which will decrease the entropy of the system. The new crystallite formations were detected at temperatures of heat treatments above 120°C, which is 20°C higher than the temperature necessary to release the hydrogen bonds. Also, this temperature is coincident with the deep change in the slopes of the linearity regions for the parameters LO and CS in the direction perpendicular to the fiber axis.

Therefore, the major structural changes in the crystalline regions will start to occur only at this temperature for this fiber. However, it is clear that the new crystallites will work as a network, promoting stabilization of the oriented extended amorphous chains at this range of temperature, making difficult its complete disorientation. The orientation of the amorphous regions (interfibrillar regions) will be somehow retained. That might be the reason why the LP, a parameter measured along the fiber axis and strongly dependent on the disorientation of these amorphous regions, will start to present a deep increase only at a temperature of heat treatment of 150°C. Thus, the LP parameter will need much more energy to show profound changes. This temperature is about 30°C above the formation of the nuclei crystallites and 50°C above the hydrogen bonds release.

Also, the results indicate that there are simultaneous improvements of the size and perfection of the new crystallites and the preexisting crystals by increasing the annealing temperatures. This fact will result in an increase of the strain level of the amorphous domains, resulting in the observed increase of the total order of the system. In addition, the global recrystallization will occur consequently in a preferred direction, as indicated by the  $\Delta n$  results (i.e., in the direction of the fiber axis). Finally, these analysis demonstrate that all of the phenomenological aspects associated with the recrystallization process are interrelated and will command the shrinkage behavior.

### *The Nylon 6.6 Fiber*

The shrinkage mechanism of the Nylon 6.6 fiber presented a less complex behavior, with no generation of nuclei crystallites during thermal annealing. This fiber presented a nearly instantaneous shrinkage at a heat-setting temperature around 70°C. As indicated in a previous discussion, that is the necessary temperature to overcome the strong hydrogen bonds for this fiber and also the starting temperature for the occurrence of the major structural changes in the amorphous and crystalline regions. These changes would be the global disorientation and recrystallization by growth and perfection of the preexisting crystals. All of these structural transformations are occurring simultaneously at the same temperature [i.e., approximately 40°C below its  $T_g$  ( $T_g \cong 115^\circ\text{C}$ )].

Although below  $T_g$ , this temperature was sufficient to give the necessary thermal energy to overcome the hydrogen bonds, thus inducing ini-

tially loss of orientation due to processing, mainly in the extended noncrystalline chains. However, the increased segmental mobility of the chains in these interfibrillar regions, as the heat-setting temperature, also increased will not promote formation of the nuclei crystallites as observed for the Nylon 6 fiber. Thus, the interfibrillar regions of the Nylon 6.6 fiber will not be experiencing any opposing thermodynamic process that would difficult further disorientation of such regions. Therefore, a conformation of lower energy will be more easily reached by these macromolecular chains.

This process will favor recrystallization only by reorganization of preexisting crystals (such as growth and perfection). Also, the intense disorientation of the amorphous regions will be interfering somehow in the orientation of the crystalline regions, allowing a recrystallization with no preferred orientation, as confirmed by the birefringence analysis.

The comparison between the two nylon fibers concerning their different response to the applied thermal annealing, was essential for us to formulate the following hypothesis: one of the main reasons for the occurrence of different shrinkage mechanisms resides in the different crystalline morphology that these fibers originally possessed before heat treatments.

As shown in a previous section of this article, the Nylon 6.6 fibers, differently from the Nylon 6, presented a double melting peak that might be representative of the fusion of the two different crystalline structures.<sup>17</sup> The temperatures of the melting peaks increased about 10°C after the annealing, remaining constant for all analyzed heat treatment temperatures. This result confirms an increase of size and perfection of these crystals. Because the characteristic double melting peaks were maintained for all heat settings, it is possible to suppose that the two crystalline structures—but larger and more perfect—were preserved. This fact will be explored later in part II.

Yet, it is possible to propose the hypothesis that the existence of these two crystalline structures for all studied annealing temperatures might be preventing the formation of the nuclei crystallites, as detected for the Nylon 6 case. It is interesting to note that the DSC thermograms revealed a tendency of the single and main melting peak of the Nylon 6 fiber to dismember in two peaks for the annealing temperatures above 120°C. Also, this temperature was coincident with the appearance of the premelting peaks, which represent the fu-

sion of the nuclei crystallite, as described previously. In addition, the observed dislocation of the premelting peak to higher temperatures as the heat-setting temperature also increased, seems to accentuate the dismembering of the main melting peak. At annealing temperature of 190°C, the premelting peak temperature (216°C) is almost coincident with the temperature (225°C) of the appearance of the second main melting peak. This fact sustains an earlier hypothesis that the crystalline structure of the Nylon 6 fiber is becoming more similar to the Nylon 6.6 fiber (i.e., with two different crystalline structures with thermal annealing). These small crystallites could be considered as nuclei for the formation of a second crystalline structure in this fiber.

## CONCLUSIONS

The studied Nylon 6 and 6.6 fibers presented different shrinkage behaviors due to thermal annealing. The Nylon 6 fiber experienced lower shrinkage than Nylon 6.6 for most of the studied annealing temperatures.

Comparison between the structural changes of the fibers due to the heat settings was essential for the understanding of the different mechanisms.

The structural changes due to thermal annealing were associated with the following phenomena: disorientation and recrystallization by nucleation of new crystallites and by growth and perfection of the existing crystals.

These phenomena were different for the analyzed fibers and were dependent on the original structural characteristics of the fibers (i.e., prior to the heat settings).

The thermal annealed Nylon 6 fiber presented a recrystallization that occurred with the formation of nuclei crystallites in the extended noncrystalline chains (interfibrillar regions) and simultaneous improvement of the size and perfection of the new crystallites and the premelting ones, as the temperature of heat treatment increased. The nuclei crystallites played a very important role in the shrinkage process of this fiber; they worked as crosslinking points, making difficult the complete disorientation of the interfibrillar regions and consequently an accentuated shrinkage. Also, this process favored recrystallization in a preferred direction of the fiber axis. The total order of the system increased accentuatedly for the heat treatments above the glass transition of the fiber.

The Nylon 6.6 fiber did not present generation of nuclei crystallites during thermal annealing. Thus, the main commanding factor of the shrinkage behavior of this fiber was the chain flexibility imparted by loosening of the hydrogen bonds at one temperature of heat treatment  $\sim 40^\circ\text{C}$  below its  $T_g$ . Therefore, this fiber experienced an instantaneous shrinkage at this temperature. Because this fiber did not experience any formation of nuclei crystallites during thermal annealing, there was no opposing mechanism that could prevent the complete disorientation of its interfibrillar regions. This fact allowed simultaneous disorientation of the crystalline regions as well. Thus, recrystallization in this case occurred only by growth and perfection of the preexisting crystals with the annealing temperature and with no preferred orientation as detected by birefringence analysis.

Finally, analysis of the DSC thermograms obtained for the fibers reinforced the hypothesis that the crystalline structure of the Nylon 6 fiber is becoming more similar to Nylon 6.6, as the temperature of the heat treatment increased. Therefore, the nuclei crystallites would be seeds for the formation of a new crystallite structure that would appear as a second main melting peak in the DSC thermogram, as observed for the Nylon 6.6 fiber. That would be the reason why the Nylon 6.6 fiber did not present formation of nuclei crystallites during thermal annealings.

This research was supported in part by Fundação Coordenação de Aperfeiçoamento de Pessoal de Nível Superior (CAPES) and in part by Fundação de Amparo à Pesquisa do Estado de São Paulo (FAPESP). The authors thank Professor Yvonne P. Mascarenhas and the technicians of the Institute of Physics of São Carlos—

USP for permitting and helping us with the utilization of their X-ray equipment. The authors also appreciate the excellent digitation work by Leine Ap. Silva.

## REFERENCES

1. N. S. Murthy, H. Minor, and R. A. Latif, *J. Macromol. Sci. Phys.*, **B26**, 427 (1987).
2. L. A. de G. Oriani and A. L. Simal, *J. Appl. Polym. Sci.*, **46**, 1973 (1992).
3. R. J. Samuels, *Structured Polymer Properties*, John Wiley and Sons, New York, 1974.
4. I. M. Fouda, M. M. El-Tonsy, and A. M. Shaban, *J. Mater. Sci.*, **26**, 5085 (1991).
5. H. J. Oswald, E. A. Turi, P. J. Harget, and Y. P. Khanna, *J. Macromol. Sci. Phys.*, **B13**, 231 (1977).
6. Y. P. Khanna, *J. Appl. Polym. Sci.*, **40**, 569 (1990).
7. M. S. Araújo and A. L. Simal, *J. Appl. Polym. Sci.*, **60**, 2437 (1996).
8. J. Gacén, F. Bernald, and J. Maillo, *Text. Chem. Col.*, **20**, 31 (1988).
9. A. L. Simal and L. A. G. Oriani, *J. Appl. Polym. Sci.*, **46**, 1987 (1992).
10. M. Hirami, *J. Macromol. Sci. Phys.*, **B23**, 347–414 (1984–1985).
11. H. W. Stakweather, Jr., P. Zoller, and G. A. Jones, *J. Polym. Sci., Phys. Ed.*, **22**, 1615 (1984).
12. P. F. Dismore and W. O. Statton, *J. Polym. Sci., Part C*, **13**, 133, 1966.
13. D. R. Subramanian, A. Venkataraman, and N. V. Bhat, *J. Macromol. Sci.*, **B18**, 177 (1980).
14. L. E. Alexander, *X-ray Diffraction Methods in Polymer Science*, Wiley Interscience, New York, 1969.
15. A. M. Hindeleh and D. J. Johnson, *Polymer*, **19**, 27 (1978).
16. D. C. Prevorsek and H. J. Oswald, in *Solid State Behavior of Linear Polyesters and Polyamides*, J. Schultz and S. Fakirov, Eds., Prentice-Hall, Englewood Cliffs, NJ, 1990.
17. J. P. Bell, *Textile Res. J.*, **42**, 292, 1972.